A&A 484, 451–455 (2008)
DOI: 10.1051/0004-6361:20079308

Astronomy & Astrophysics

XMM-Newton observations of the Small Magellanic Cloud: X-ray outburst of the 6.85 s pulsar XTE J0103-728⋆

F. Haberl and W. Pietsch

Max-Planck-Institut für extraterrestrische Physik, Giessenbachstraße, 85748 Garching, Germany
e-mail: [fwh;wnp]@mpe.mpg.de

Received 21 December 2007 / Accepted 11 March 2008

ABSTRACT

Context. A bright X-ray transient was seen during an XMM-Newton observation in the direction of the Small Magellanic Cloud (SMC) in October 2006.
Aims. The data from the European Photon Imaging Cameras (EPIC) allow us to accurately locate the source and to investigate its temporal and spectral behaviour.
Methods. We extracted X-ray spectra covering 0.2−10 keV and pulse profiles in different energy bands from the EPIC data.
Results. The detection of 6.85 s pulsations in the EPIC-PN data unambiguously identifies the transient with XTE J0103-728, discovered as 6.85 s pulsar by the Rossi X-ray Timing Explorer. The X-ray light curve during the XMM-Newton observation shows flaring activity of the source with intensity changes by a factor of two within 10 min. Modelling of pulse-phase averaged spectra with a simple absorbed powerlaw indicates systematic residuals, which can be accounted for by a second emission component. From a model implying blackbody emission due to reprocessing by optically-thick material in the inner accretion disk, we estimate the inner disk radius to ∼160 km. The photon index of the powerlaw of ∼0.4 indicates a relatively hard spectrum. The 0.2−10 keV luminosity was 2×10^{37} erg s^{-1} with a contribution of ∼3% from the disk-blackbody component. A likely origin for the excess emission is reprocessing of hard X-rays from the neutron star by optically-thick material near the inner edge of an accretion disk. From a timing analysis we determine the pulse period to 6.85401(1) s, indicating an average spin-down of ∼0.0017 s per year since the discovery of XTE J0103-728 in May 2003.
Conclusions. The X-ray properties and the identification with a Be star confirm XTE J0103-728 as Be/X-ray binary transient in the SMC.

Key words. Galaxy: stellar content – stars: emission-line, Be – stars: neutron – X-rays: binaries – galaxies: Magellanic Clouds

1. Introduction

The transient pulsar XTE J0103-728, with a period of 6.8482 ± 0.0007 s was discovered during observations of the Small Magellanic Cloud (SMC) with the Rossi X-ray Timing Explorer (RXTE). The pulsations were detected on 2003, Apr. 29, May 7, May 15 and May 19, but not on Apr. 24 and May 28 (Corbet et al. 2003), suggesting an X-ray outburst that lasted about three to four weeks. This behaviour is characteristic for Be/X-ray binaries undergoing a type II outburst caused by the ejection of matter from the Be star and enhanced accretion onto a compact object, in most cases a neutron star (Negueruela 1998). Shorter outbursts (type I) with a duration of a few days are often separated by the orbital period of the binary system. They generally occur close to the time of periastron passage of the neutron star when the neutron star approaches the circumstellar disc of the Be star (see, e.g., Okazaki & Negueruela 2001).

Be/X-ray binaries form the major class of high mass X-ray binaries (HMXBs). In the remaining systems – the supergiant HMXBs – the compact object accretes matter from the fast stellar wind of an early-type O or B supergiant star. In the SMC more than 60 Be-HMXBs are known, while only one HMXB is established as a supergiant system (SMC X-1). Recent reviews of the optical and X-ray properties of these systems can be found in Coe et al. (2005) and Haberl & Pietsch (2004), respectively.

The X-ray transient XTE J0103-728 is one of several Be/X-ray binary candidates in the SMC that were discovered through their pulsations with RXTE. This non-imaging instrument is able to monitor the activity of pulsars in the SMC (Laycock et al. 2005), but provides only a coarse determination of their sky coordinates. The latter hampers the optical identification and final confirmation of the HMXB nature of the pulsars. We detected the pulsar XTE J0103-728 in X-ray outburst during an XMM-Newton observation of RX J0103.8−7254, a candidate super-soft X-ray source in the direction of the SMC discovered by ROSAT. The precise localisation in the EPIC images allowed us to identify the optical counterpart of XTE J0103-728, which shows optical brightness and colours consistent with a Be star (see Haberl et al. 2007). Analysis of the data of the counterpart from the Massive Compact Halo Object project (MACHO) and the Optical Gravitational Lensing Experiment (OGLE) reveals long-term variations in the optical light curve (Schmidtke & Cowley 2007) on timescales of 620 to 660 days which are not periodic, suggesting that they are related to the Be phenomenon and not to the binary orbit (McGowan et al. 2008). Here we present a temporal and spectral analysis of the EPIC data of XTE J0103-728 obtained in October 2006.

2. Observations and data reduction

We observed an X-ray transient as the brightest source in the field of view of the European Photon Imaging Cameras (EPIC) during an XMM-Newton (Jansen et al. 2001) observation in the

⋆ Based on observations with XMM-Newton, an ESA Science Mission with instruments and contributions directly funded by ESA Member states and the USA (NASA).

Table 1. XMM-Newton EPIC observations of XTE J0103-728.

Observation ID	Pointing direction RA	Dec (J2000.0)	Sat. Rev.
0402000101	01 03 52.2	–72 54 28	1248
EPIC[1] instrument configuration	Start time 2006-10-03 (UT)	End time	Net exposure ks
PN FF thin	00:31:21	06:13:06	17.72
M1 FF thin	00:08:39	06:12:46	21.32
M2 FF thin	00:08:39	06:12:51	21.30

[1] FF thin: full frame CCD readout mode with 73 ms frame time for PN and 2.6 s for MOS; thin optical blocking filter.

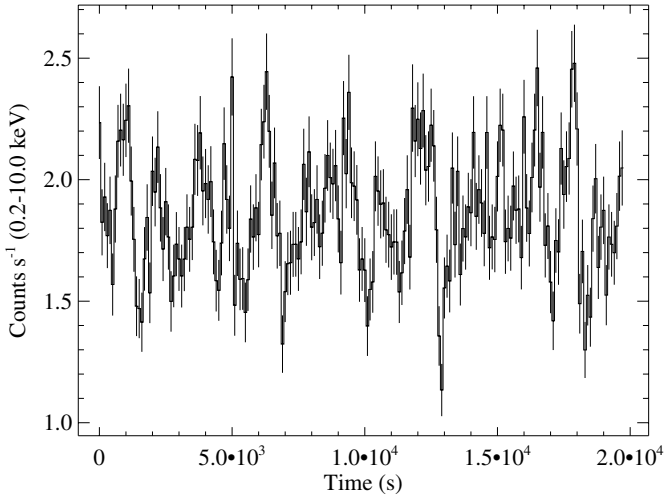

Fig. 1. Broad-band EPIC-PN light curve of XTE J0103-728. The data is background subtracted and binned to 100 s with time 0 corresponding to MJD 54011.02678.

direction of the SMC, as summarised in Table 1. We operated the EPIC-MOS (Turner et al. 2001) and EPIC-PN (Strüder et al. 2001) cameras in imaging mode, covering the source at an off-axis angle of about 12′. Background flaring activity was negligible and we used the full exposure time for our analysis. For the data processing we used the XMM-Newton Science Analysis System (SAS) version 7.1.0 supported by tools from the FTOOL package together with XSPEC version 11.3.2p for spectral modelling.

3. Results

We performed a source detection analysis of the EPIC images using standard maximum likelihood procedures from the SAS package. After applying a bore-sight correction with a background AGN and a foreground star in the field of view we determined the position of the brightest source to RA = $01^h02^m53^s.39$ and Dec = –72°44′34.″6 (J2000.0) with a remaining systematic uncertainty of 1.1″ (1σ). No source at this position was seen in ROSAT observations (Haberl et al. 2000; Sasaki et al. 2000).

During the XMM-Newton observation, the source showed strong flaring activity with intensity changes by a factor of ∼2 within 10 min. This is illustrated in Fig. 1 where the broad-band EPIC-PN light curve is shown. A Fourier analysis of the EPIC-PN data clearly revealed the presence of 6.85 s pulsations in the X-ray flux, which identifies the bright EPIC source with XTE J0103-728. We saw no significant signal of higher harmonics. Using a folding technique, we determined the pulse period to $(6.85401 \pm 1 \times 10^{-5})$ s (1σ error). This corresponds to an average spin-up of ∼0.0017 s per year between the RXTE and the XMM-Newton observations, 3.4 years apart.

The precise position allowed us to identify the optical counterpart (Haberl et al. 2007), which is included in the *UBVR* CCD Survey of the Magellanic Clouds (Massey 2002), the Magellanic Clouds Photometric Survey (MCPS, Zaritsky et al. 2002) and in the OGLE BVI photometry catalogue (Udalski et al. 1998) as summarised in Table 2. Optical brightness, colours, and temporal properties are all consistent with a Be star (Schmidtke & Cowley 2007; McGowan et al. 2008), confirming the Be/X-ray binary nature of XTE J0103-728.

The X-ray light curves were folded in standard EPIC energy bands as shown in Fig. 2. We derived hardness ratios with HR1 = (R2 – R1)/(R2 + R1), HR2 = (R3 – R2)/(R3 + R2), and HR3 = (R4 – R3)/(R4 + R3) with RN denoting the background-subtracted count rate in band N (starting with band 1 at the lowest energies). Computed from count rates below 1 keV, HR1 is more sensitive to changes in absorption column density, while HR2 and HR3 can be used as indicator for variations in the shape of the intrinsic source spectrum up to 4.5 keV. The three hardness ratios plotted versus pulse phase are shown in Fig. 3.

The pulse profile of XTE J0103-728 is highly structured and strongly energy dependent. The pulsed fraction decreases with increasing energy up to ∼4.5 keV, but is higher again above ∼4.5 keV. Several features in the folded light curves strongly change their appearance in the various energy bands. The intensity maximum in the 0.2–0.5 keV band, e.g., reverses to a minimum at high energies above 4.5 keV and the sharp minima seen between 1.0–2.0 keV are largely smeared out at energies above 4.5 keV. The hardness ratio HR1 indicates a relatively smooth change in the low-energy part of the spectrum, either due to variations in column density or to a low-energy spectral component. Variations are also seen in HR2 and similarly in HR3, which suggest changes in the overall spectral shape.

We extracted pulse-phase averaged EPIC spectra for PN (single + double pixel events, PATTERN 0–4) and MOS (PATTERN 0–12) excluding bad CCD pixels and columns (FLAG 0). Due to the large off-axis angle we used an elliptical source extraction region which was cut in the case of EPIC-PN by the nearby CCD border. The fluxes derived from the PN spectrum were systematically lower than those from the MOS, probably due to under-correction of the flux losses. Therefore, we report fluxes and luminosities (see below) derived from the MOS spectra. The three EPIC spectra were simultaneously fit with the same model allowing for a constant normalisation factor between the spectra. The spectra show an extremely flat distribution in the EPIC energy band which indicates a very hard spectrum. We included two absorption components in our spectral modelling, accounting for the Galactic foreground absorption (with a fixed hydrogen column density of 6×10^{20} cm^{-2} and with elemental abundances from Wilms et al. 2000) and the SMC absorption (with column density as free parameter in the fit and with metal abundances reduced to 0.2 as typical for the SMC; Russell & Dopita 1992). A bremsstrahlung model is not able to reproduce the flat spectral distribution, while a powerlaw (PL) yields a formally acceptable fit (see Table 3 and Fig. 4). However, the residuals indicate some systematic deviation from a powerlaw model. Using a broken powerlaw yields a good fit with $\chi^2_r = 1.02$ with a steeper powerlaw index below 2 keV than above, which indicates excess

Table 2. Optical identification of XTE J0103-728.

Catalogue	RA and Dec (J2000.0)	Vmag	$B-V$	$U-B$	$V-R$	$V-I$
UBVR	$01^h02^m53\overset{s}{.}30$ $-72°44'34\overset{''}{.}9$	14.59	−0.08	−0.96	−0.90	–
MCPS	$01^h02^m53\overset{s}{.}39$ $-72°44'34\overset{''}{.}7$	14.99	−0.19	−1.12	–	−0.10
OGLE	$01^h02^m53\overset{s}{.}29$ $-72°44'34\overset{''}{.}8$	14.68	−0.12	–	–	0.04

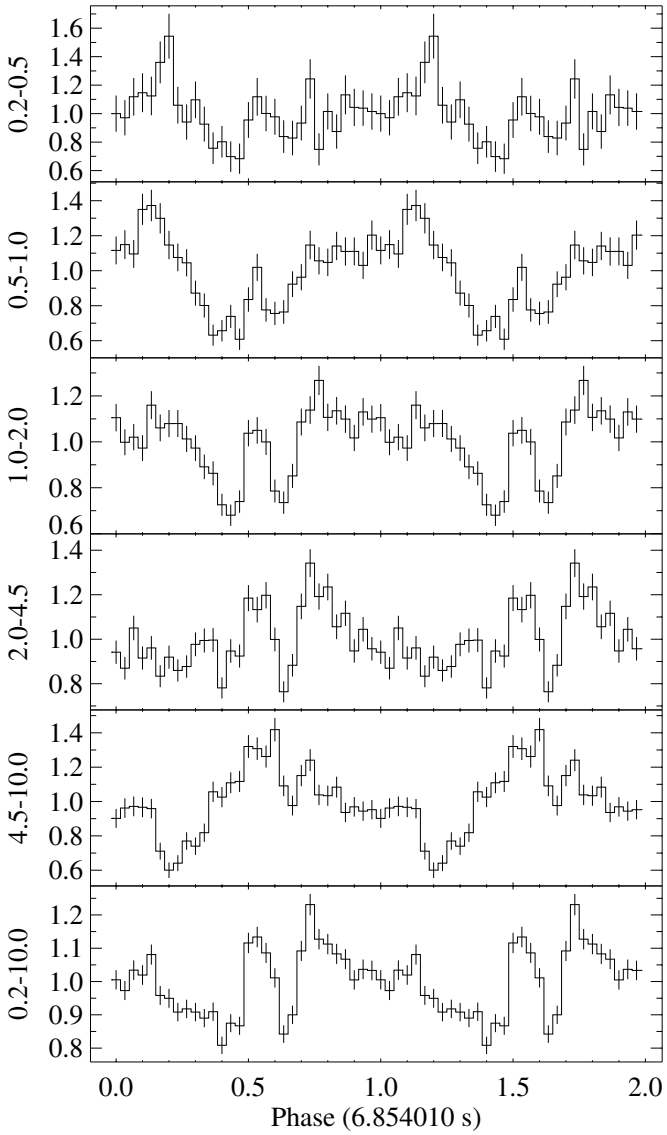

Fig. 2. Folded EPIC-PN light curves in the standard EPIC energy bands. The panels show the pulse profiles for the different energies specified in keV. The intensity profiles are background subtracted and normalised to the average count rate (in cts s^{-1}: 0.103, 0.268, 0.482, 0.530, 0.466, 1.86 *from top to bottom*).

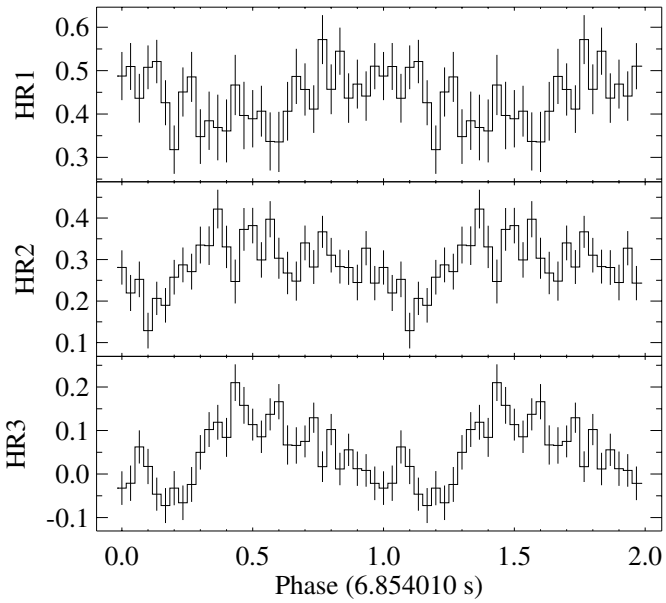

Fig. 3. Hardness ratios HR1 = [R(0.5–1.0)–R(0.2–0.5)]/[R(0.2–1.0)]; HR2 = [R(1.0–2.0)–R(0.5–1.0)]/[R(0.5–2.0)]; and HR3 = [R(2.0–4.5)–R(1.0–2.0)]/[R(1.0–4.5)] derived from the folded EPIC-PN light curves shown in Fig. 2. R denotes the count rates as a function of pulse phase in the given energy bands (in keV).

emission below ∼2 keV. For a better description of this excess, we add different model components to the simple powerlaw.

Two different kinds of low-energy excess seen in the X-ray spectra of HMXBs were reported in the literature. A soft emission component from Be-HMXBs is interpreted as reprocessed X-ray emission and may originate from different places in the binary system (Hickox et al. 2004). The Be-HMXB RX J0103.6−7201 (with 1323 s the pulsar with the longest period known in the SMC) showed during one XMM-Newton observation a highly-absorbed powerlaw component and a completely disentangled soft component. The soft component was modelled as thermal plasma emission (Haberl & Pietsch 2005). Using a thermal plasma emission component in combination with the powerlaw (PL+MEKAL) yields an improved fit for XTE J0103-728 (Table 3), but a temperature of >1.3 keV much higher than typical values found for other sources (0.15 keV for RX J0103.6−7201). This is inconsistent with a very soft emission component present below ∼1.3 keV, similar to that observed from RX J0103.6−7201. A relatively hot component with a characteristic blackbody temperature of ≳1 keV and a small emission area with radius ≲0.5 km was found in two persistent Be pulsars (e.g., RX J0146.9+6121; La Palombara & Mereghetti 2006) and was interpreted as emission from the hot polar caps of the accreting neutron star. Adding a blackbody component to the modelling of XTE J0103-728 (PL+BB), we obtain a lower temperature around 0.25 keV (Table 3) and a larger emission area (radius 30.8 km), which is inconsistent with the surface of the neutron star. The inferred radius might indicate emission from the inner accretion disk and therefore, we added a multi-temperature blackbody model (diskbb in XSPEC) to the powerlaw model (PL + DB in Table 3). Again, the fit is acceptable with a temperature of the inner disk of 0.36 keV (Table 3) and a lower limit for the inner disk radius $R_{\rm in}$ of ∼13.3 km (assuming a disk inclination angle cos θ of 1.0; $R_{\rm in} \propto 1/\sqrt{\cos\theta}$). The disk-blackbody component contributes 3.0% to the total luminosity in the 0.2−10.0 keV band. The EPIC spectra together with the best

Table 3. Spectral fit results.

Model[1]	SMC N_H [10^{20} cm^{-2}]	γ	kT [keV]	Flux[2] erg cm^{-2} s^{-1}	L_x[3] erg s^{-1}	χ^2_r/d.o.f.
PL	2.44 ± 0.85	0.54 ± 0.02	–	4.55×10^{-11}	1.98×10^{37}	1.21/830
PL+BB	7.1 ± 1.6	0.42 ± 0.02	0.242 ± 0.024	4.75×10^{-11}	2.08×10^{37}	1.02/828
PL+MEKAL	9.4 ± 1.5	0.35 ± 0.08	$1.7^{+1.9}_{-0.4}$	4.79×10^{-11}	2.11×10^{37}	1.04/828
PL+DB	11.3 ± 2.3	0.41 ± 0.04	0.36 ± 0.06	4.77×10^{-11}	2.10×10^{37}	1.02/828

[1] For definition of spectral models see text. [2] Observed 0.2–10.0 keV flux. [3] Source intrinsic X-ray luminosity in the 0.2–10.0 keV band (corrected for absorption) for a distance to the SMC of 60 kpc (Hilditch et al. 2005).

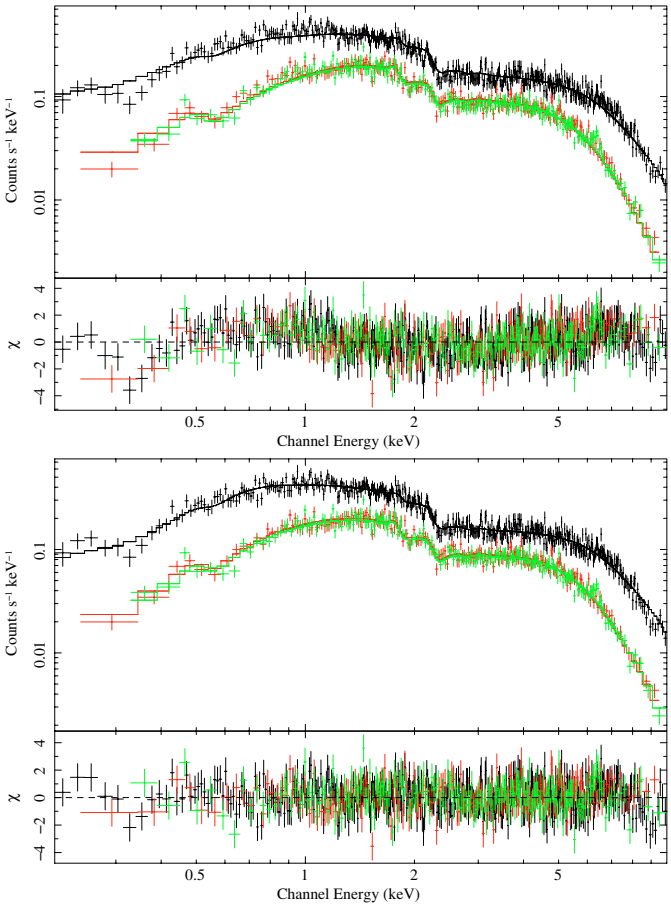

Fig. 4. EPIC spectra of XTE J0103-728. EPIC-PN is shown in black and EPIC-MOS in red (M1) and green (M2) (both grey in black and white representation). The histograms show the best-fit model: (*top*) an absorbed powerlaw and (*bottom*) an absorbed two-component model with multi-temperature disk and powerlaw emission (PL+DB in Table 3).

fit PL + DB model are shown in Fig. 4. In Table 3, we summarise the characteristic model parameters and give observed fluxes and luminosities.

4. Discussion

After its discovery with RXTE in April 2003, we detected the 6.85 s pulsar XTE J0103-728 in X-rays for the first time with imaging instruments, which allowed us to better localise the source and identify the optical counterpart. During the XMM-Newton observation in October 2006 the source was seen in outburst with a luminosity of $\sim2\times10^{37}$ erg s^{-1} in the 0.2−10.0 keV band. During the observation the source strongly varied in intensity with changes by a factor of two within ten minutes. Pulse profiles obtained by folding the data from the EPIC-PN detector in different energy bands with 30 phase bins (corresponding to 228.5 ms per phase bin) are highly structured. The fast intensity variations indicate that the bulk of the emission originates close to the neutron star surface and suggests a complicated emission geometry with narrow beams contributing to the X-ray emission at various neutron star spin phases with energy dependent amplitudes.

Deviations from a powerlaw model in the phase averaged EPIC spectra suggest an additional emission component mainly contributing to energies below ∼1.5 keV. This component is harder than the soft component seen in other Be-HMXBs in the SMC, which can be modelled as thermal plasma emission with $kT \sim 0.15$ keV (see, e.g., RX J0103.6−7201; Haberl & Pietsch 2005). On the other hand, the excess emission in the spectra of XTE J0103-728 is softer than the hot blackbody component seen in XMM-Newton spectra of two persistent Be-HMXBs in the Milky Way (La Palombara & Mereghetti 2006, 2007), which is interpreted as emission from hot polar caps of the neutron star. When modelled as blackbody emission, the large inferred emission area (with radius ∼30 km) for XTE J0103-728 is incompatible with an origin on the neutron star surface.

In their work on the origin of the soft excess in X-ray pulsars, Hickox et al. (2004) conclude that for luminous X-ray pulsars ($\gtrsim10^{38}$ erg s^{-1}) the soft excess can only be explained by reprocessing of hard X-rays from the neutron star by optically-thick material. At intermediate luminosity ($\sim10^{37}$ erg s^{-1}) other processes, such as emission from photo-ionised or collisionally-heated gas, can also contribute. The spectra of XTE J0103-728 do not show significant line emission suggesting that in this source the excess emission is mainly caused by reprocessing in optically-thick material, most likely located near the inner edge of an accretion disk. The small contribution of the soft component (∼3%) to the total luminosity is consistent with such a model. Using blackbody or disk-blackbody models to estimate the inner disk radius yields relatively small values with ∼31 km blackbody radius and a lower limit of ∼13 km for the inner disk radius inferred from the disk-blackbody model. In the latter case, a value more consistent with the typical radius of the neutron star magnetosphere (10^8 cm) can only be obtained for a disk inclination close to 90°, which should probably result in a higher absorption of the powerlaw component. Hickox et al. (2004) suggest estimating the inner disk radius with $R^2_{in} = L_x/(4\pi\sigma T^4)$; with $L_x = 2\times10^{37}$ erg s^{-1} and $kT = 0.24$ keV for XTE J0103-728, this yields a realistic value of 160 km for R_{in}.

The luminosity of the soft component seen from RX J0103.6−7201 is strongly correlated with the total source luminosity over at least a factor of ten variation in source intensity. At a maximum of $\sim6.4\times10^{36}$ erg s^{-1}, RX J0103.6−7201

is still a factor of ~3 below the luminosity of XTE J0103-728 during its October 2006 outburst. This is consistent with the conclusions of Hickox et al. (2004), that for lower luminosities emission from diffuse, optically-thin gas dominates. Which of the emission components becomes visible in the X-ray spectra of Be-HMXBs certainly depends not only on source luminosity but also on geometric effects.

Acknowledgements. The XMM-Newton project is supported by the Bundesministerium für Wirtschaft und Technologie/Deutsches Zentrum für Luft- und Raumfahrt (BMWI/DLR, FKZ 50 OX 0001) and the Max-Planck Society.

References

Coe, M. J., Edge, W. R. T., Galache, J. L., & McBride, V. A. 2005, MNRAS, 356, 502
Corbet, R. H. D., Markwardt, C. B., Marshall, F. E., et al. 2003, The Astronomer's Telegram, 163, 1
Haberl, F., & Pietsch, W. 2004, A&A, 414, 667
Haberl, F., & Pietsch, W. 2005, A&A, 438, 211
Haberl, F., Filipović, M. D., Pietsch, W., & Kahabka, P. 2000, A&AS, 142, 41
Haberl, F., Pietsch, W., & Kahabka, P. 2007, The Astronomer's Telegram, 1095, 1
Hickox, R. C., Narayan, R., & Kallman, T. R. 2004, ApJ, 614, 881
Hilditch, R. W., Howarth, I. D., & Harries, T. J. 2005, MNRAS, 357, 304
Jansen, F., Lumb, D., Altieri, B., et al. 2001, A&A, 365, L1
La Palombara, N., & Mereghetti, S. 2006, A&A, 455, 283
La Palombara, N., & Mereghetti, S. 2007, A&A, 474, 137
Laycock, S., Corbet, R. H. D., Coe, M. J., et al. 2005, ApJS, 161, 96
Massey, P. 2002, ApJS, 141, 81
McGowan, K. E., Coe, M. J., Schurch, M. P. E., et al. 2008, MNRAS, 384, 821
Negueruela, I. 1998, A&A, 338, 505
Okazaki, A. T., & Negueruela, I. 2001, A&A, 377, 161
Russell, S. C., & Dopita, M. A. 1992, ApJ, 384, 508
Sasaki, M., Haberl, F., & Pietsch, W. 2000, A&AS, 147, 75
Schmidtke, P. C., & Cowley, A. P. 2007, The Astronomer's Telegram, 1181, 1
Strüder, L., Briel, U., Dennerl, K., et al. 2001, A&A, 365, L18
Turner, M. J. L., Abbey, A., Arnaud, M., et al. 2001, A&A, 365, L27
Udalski, A., Szymanski, M., Kubiak, M., et al. 1998, Acta Astron., 48, 147
Wilms, J., Allen, A., & McCray, R. 2000, ApJ, 542, 914
Zaritsky, D., Harris, J., Thompson, I. B., Grebel, E. K., & Massey, P. 2002, AJ, 123, 855